



The Society shall not be responsible for statements or opinions advanced in papers or discussion at meetings of the Society or of its Divisions or Sections, or printed in its publications. Discussion is printed only if the paper is published in an ASME Journal. Authorization to photocopy material for internal or personal use under circumstance not falling within the fair use provisions of the Copyright Act is granted by ASME to libraries and other users registered with the Copyright Clearance Center (CCC) Transactional Reporting Service provided that the base fee of \$0.30 per page is paid directly to the CCC, 27 Congress Street, Salem MA 01970. Requests for special permission or bulk reproduction should be addressed to the ASME Technical Publishing Department.

Copyright © 1997 by ASME

All Rights Reserved

Printed in U.S.A.

## INTERMITTENT FLOW AND THERMAL STRUCTURES OF ACCELERATING TRANSITIONAL BOUNDARY LAYERS, PART 2: FLUCTUATION QUANTITIES



Ting Wang and F. Jeffrey Keller\*

Department of Mechanical Engineering  
Clemson University  
Clemson, South Carolina, U.S.A.

### ABSTRACT

The conditionally sampled fluctuation quantities of non-accelerating and accelerating heated transitional boundary layers were analyzed. The results indicated that the values of  $u'$ ,  $v'$ ,  $\overline{uv}$ , and  $\overline{ut}$  in the turbulent part of the transitional flow were higher than those values in the fully-developed turbulent flow. These higher values were believed to be manifestations of the vigorous activities involved in the transition process. The contributions to the unconditioned  $u'$  by "mean-step" change due to the alternating behavior between turbulent and non-turbulent flows are about 20% in the near-wall region, but are negligible for  $Y^+ > 30$ . The turbulent part  $\overline{uv}$  values are higher than the fully turbulent and unconditioned values in the inner boundary layer but lower in the outer boundary layer. The mean-step change has negligible effect on unconditioned  $\overline{uv}$  values. As acceleration increases, both  $u'$  and  $t'$  in the turbulent part are suppressed; however, turbulent part  $u'$  is still higher than the unconditioned  $u'$ . Acceleration promotes streamwise Reynolds heat flux ( $\overline{ut}$ ) transport in both turbulent and non-turbulent parts. A second peak of the turbulent part  $\overline{ut}$  occurs at around  $Y^+ = 120$  as acceleration increases. The turbulent part eddy viscosity values are much lower than those in the fully turbulent flow.

### NOMENCLATURE

- $C_p$  - specific heat
- $K$  - pressure gradient parameter,  $\frac{v}{U_\infty^2} \frac{dU_\infty}{dx}$
- $q''_w$  - wall heat flux
- $Re$  - Reynolds number
- $T$  - instantaneous temperature
- $t'$  - rms value of temperature fluctuations
- $u', v'$  - rms values of velocity fluctuations

- $u_\tau$  - friction velocity,  $\sqrt{\tau_w / \rho}$
- $U^+$  -  $\overline{U} / u_\tau$
- $\overline{uv}$  - Reynolds shear stress
- $\overline{ut}$  - streamwise Reynolds heat flux
- $Y^+$  -  $yu_\tau / \nu$
- Greek
- $\delta^*$  - boundary layer thickness at  $0.995 U_\infty$
- $\epsilon_M$  - turbulent (or eddy) viscosity
- $\Gamma$  - intermittency factor
- $\nu$  - kinematic viscosity
- $\rho$  - density
- $\tau_w$  - shear stress on the wall

### Subscripts:

- $\infty$  - free-stream value
- $t$  - turbulent
- $nt$  - non-turbulent

### INTRODUCTION

The results of Part 1 provided conditionally sampled mean values in the turbulent and non-turbulent parts in the intermittent, transitional boundary layers. Part 2 will focus on the fluctuation quantities. These fluctuation quantities provided information regarding the production of turbulent kinetic energy, turbulent shear stress transports, and turbulent heat flux transport, which are necessary for modeling turbulence and verifying CFD results. The instantaneous traces of velocity or turbulence shear stress can also serve as an important database for verifying the results from direct numerical analysis (DNS).

Blair (1992) employed an ensemble-averaging technique to analyze the turbulent burst profiles of randomly passing turbulent patches in accelerating boundaries with intense free-stream

\*F.J. Keller is currently working at Accuracy Microsensors, Inc. Pittsford, New York.

turbulence. He discovered that as much as one-half of the streamwise-component unsteadiness, and much of the apparent anisotropy observed near the wall, was not produced by turbulence, but by the steps in velocity between the turbulent and non-turbulent zones of flow. His results regarding the turbulence kinetic energy indicated that the non-turbulent part preserved the characteristics of a highly disturbed laminar boundary layer all the way through transition.

The objectives of this paper are to provide a detailed analysis of the conditionally sampled fluctuation quantities in heated transitional boundary layers and investigate the effects of streamwise acceleration on the development of these fluctuation quantities in the transition process.

## RESULTS AND DISCUSSION

The effects of acceleration on the unconditioned flow and thermal structures have been discussed by Keller and Wang (1996). This paper will focus on the conditionally sampled results.

**Streamwise and Cross-Stream Velocity Fluctuations ( $u'$  and  $v'$ ).** For the Reynolds normal stresses, the unconditioned values obtained in the transitional boundary layer are a combination of the non-turbulent and turbulent portions plus the intermittent alternation between the non-turbulent and turbulent mean values, as shown below.

$$u'^2 = \Gamma u_t'^2 + (1-\Gamma)u_{nt}'^2 + \Gamma(1-\Gamma)(\bar{U}_t - \bar{U}_{nt})^2 \quad (1)$$

The first term and second term on the right side of equation 1 can be directly obtained by conditional sampling and are termed non-turbulent contribution and turbulent contribution, respectively. The last term can be calculated from the conditionally sampled data. It is commonly referred to as the "mean-step contribution" and has been speculated as the cause of the peak values of unconditioned  $u'$  found in the transitional boundary layer, which exceed the peak values found in a fully turbulent boundary layer (Schubauer and Klebanoff, 1956). The qualitative value of this "mean-step contribution" may be inferred by comparing the  $u'$  values obtained in the non-turbulent and turbulent portions to the unconditioned result. Note, as previously discussed, that the intermittency drops off rapidly at the edge of the boundary layer resulting in fewer turbulent readings. Too few points in this region for the turbulent portion result in a large scatter in the data. Therefore, if the intermittency in the outer boundary layer region of turbulent portion dropped below 0.005 the data were omitted from presentation. The conditionally sampled results of  $u'$  for the baseline case are shown in Fig. 1. The non-turbulent portion exhibits a peak intensity of 7.5% at  $Y^+ \approx 35$  ( $y/\delta^* \approx 1.3$ ) for station 05 ( $\Gamma = 0.05$ ), which is slightly below the 8% peak value for the unconditioned result which occurs at the same  $Y^+$  location. The maximum value of  $u'$  in the turbulent part is 16% and is greater than the 8% reached for the unconditioned result, as well as the 10% value of the fully turbulent flow at station 13 for the same  $Y^+$  location. For station 06 ( $\Gamma = 0.50$ ) the peak intensity for the non-turbulent portion increases to 9.5%. The peak magnitude for the unconditioned result is 16% at this station and occurs closer to the wall at  $Y^+ \approx 15$  ( $y/\delta^* \approx 0.3$ ). The peak magnitude in  $u'$  for the turbulent portion for station 06 increases to 18.5% and still exceeds the unconditioned value. At station 6 in Fig. 1, the individual contributions from turbulent, non-turbulent, and mean-

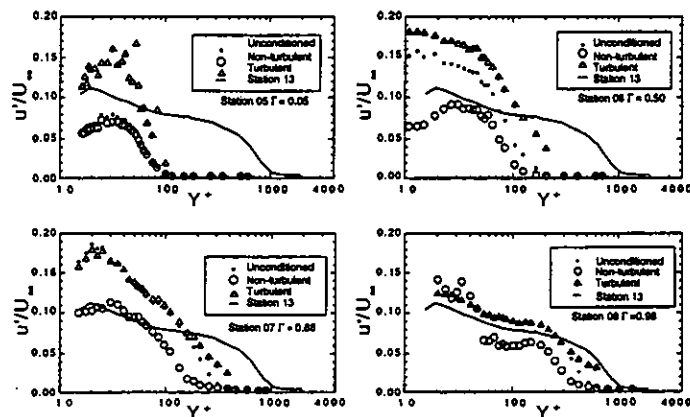


Fig. 1 Conditionally sampled  $u'$  for the baseline case.

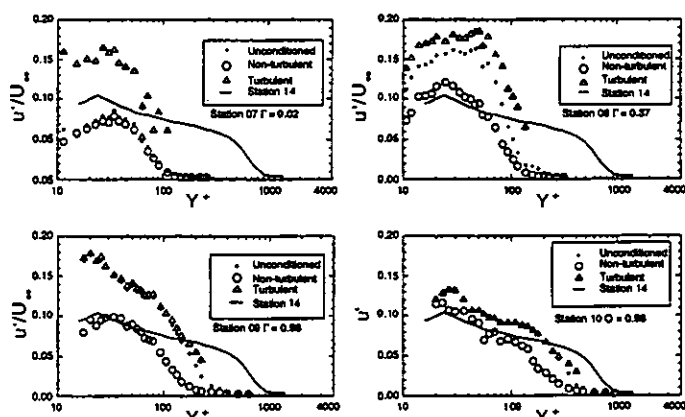


Fig. 2 Conditionally sampled  $u'$  for the K1 case.

step change to the unconditioned  $u'$  in eq. 1 are 64%, 13%, and 23% at the 3rd data point ( $Y^+ = 14.9$ ); 73%, 23%, and 4% at the 6th point ( $Y^+ = 26.8$ ); 79%, 19%, and 2.2% at the 14th point ( $Y^+ = 58.6$ ). It is clear that the turbulent part is the major term. The non-turbulent and mean-step change terms are minor terms that actually pull down the turbulent part  $u'$  values. Therefore, the unconditioned  $u'$  values become lower than the turbulent part values. The contribution from the mean-step change to  $(u')^2$  is about 23% and about 14% to  $u'$  value in the near wall region. This mean-step contribution drastically reduces as  $Y^+ > 30$ .

In the late transition region, stations 07 through 08, the peak intensity in the non-turbulent part continues to increase in magnitude. At station 07 ( $\Gamma = 0.88$ )  $u'$  in the turbulent portion is slightly below the unconditioned result, indicating a contribution from the mean-step alternation. For station 08 ( $\Gamma = 0.98$ ), the peak intensity in  $u'$  for the non-turbulent portion exceeds both the turbulent and unconditioned values near the wall. Kuan and Wang (1990) observed a similar occurrence in the late transition region and determined it was a direct result of large magnitude low frequency unsteadiness (not turbulence) in the non-turbulent intervals between the turbulent spots. Sohn et al. (1989) had a similar observation. The near-wall peak of turbulent portion decreases in magnitude from station 07 to station 08. This decrease of  $u'$  in the late transition region is most probably caused by the

effects of viscous dissipation. The conditionally sampled results of  $u'$  indicate that large magnitudes observed in the transition region are a direct result of the turbulent fluctuations in the turbulent portion, and the mean-step contribution is not a major factor. Similar observations were made by Kuan et al. (1989), Kim et al. (1989), Sohn and Reshatko (1991), and Blair (1992). These results suggest that the level of turbulent activity indicated by the unconditioned values in the transitional boundary layer is not an accurate measure of the true turbulent activity and that turbulence models using fully turbulent boundary layers to model the transport processes occurring in the turbulent spots require correction.

The conditionally sampled  $u'$  profiles for the accelerating cases are shown in Figs. 2 and 3. An interesting difference occurs between the non-turbulent portions of the accelerating cases and the baseline case. For the baseline case, the peak magnitude of  $u'$  in the non-turbulent portion increases from station 05 ( $\Gamma = 0.05$ ) up through station 07 ( $\Gamma = 0.88$ ). For the K1 case, the peak magnitude of  $u'$  in the non-turbulent portion increases from 8% at station 07 ( $\Gamma = 0.02$ ) to 12.5% at station 08 ( $\Gamma = 0.37$ ) and then decreases to 10.5% by station 09 ( $\Gamma = 0.82$ ). For the K2 case, the non-turbulent  $u'$  peak magnitude increases from 7.5% at station 07 ( $\Gamma = 0.01$ , not shown) to 13% at station 08 ( $\Gamma = 0.07$ ). The peak magnitude then decreases to 12% at station 09, finally to about 9% at station 10 ( $\Gamma = 0.37$ ) and is maintained about 9% to 10% through station 13 ( $\Gamma = 0.93$ ). This evolution of the peak value of  $u'$  indicates that as  $K$  increases,  $u'$  of the non-turbulent portion is suppressed at an earlier stage. This is consistent with the results of Schubauer and Skramstad (1947) which showed a favorable pressure gradient damps boundary layer non-turbulent oscillations in a pre-transitional boundary layer and may also suggest that this damping effect continues through the transition process.

The results for  $u'$  in the turbulent portions are similar to the baseline case. The  $u'$  values are greater than the unconditioned values in the early transition region through  $\Gamma = 0.37$  for both K1 and K2 cases. In the late transition region ( $\Gamma > 0.6$ ) the unconditioned values of  $u'$  slightly exceed the values in the turbulent portion in the near wall region indicating a mean-step contribution. This is especially noticed for station 12 of the K2 case shown in Fig. 3. As with the baseline case, the level of turbulent energy indicated by the turbulent portion in the accelerating transitional boundary layer is very different from the turbulence energy in the fully turbulent flow.

The conditionally sampled cross-stream fluctuations,  $v'$ , for the baseline case is shown in Fig. 4. There are two interesting observations. For the non-turbulent portion, the peak of  $v'$  increases from approximately 0.6% at station 05 ( $\Gamma = 0.05$ ) to 1% at station 06 ( $\Gamma = 0.50$ ) and finally to 2% at station 08 ( $\Gamma = 0.98$ ). This increase in  $v'$  as the transition process develops is most likely caused by the presence of amplified oscillations still present in the boundary layer and by the relaxation period (calm region) after the passage of a turbulent spot, since part of the low-frequency oscillations in the calm region is grouped into the non-turbulent portions. For the turbulent portion, the  $v'$  magnitude reaches the fully turbulent value by station 06 ( $\Gamma = 0.50$ ). As transition proceeds, the location of the peak magnitude migrates closer to the wall but the absolute magnitude of the peak value changes very little.

The conditionally sampled  $v'$  profiles for the accelerating cases are shown in Figs. 5 and 6. The effect of increasing  $K$  on  $v'$  in

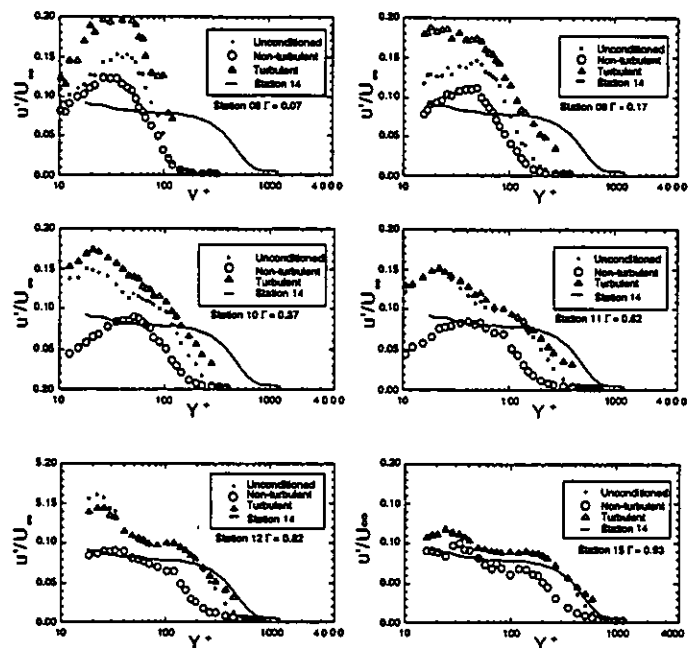


Fig. 3 Conditionally sampled  $u'$  for the K2 case.

the non-turbulent portion is similar to the effect on  $u'$  (i.e., an applied favorable pressure gradient suppresses the velocity fluctuations in the non-turbulent portion and that this suppression is greater and occurs earlier in the transition process as the pressure gradient increases). The turbulent portion of  $v'$  for all three cases is never exceeded by the unconditioned values. This is due to the mean value of the cross-stream velocity,  $\bar{v}$ , being near zero for both the turbulent and non-turbulent portions. There is no significant mean-step contribution.

**Reynolds Shear Stress ( $\overline{uv}$ ).** The reconstruction formula for the Reynolds shear stress is given as:

$$\overline{uv} = \Gamma \overline{uv}_t + (1 - \Gamma) \overline{uv}_{nt} + \Gamma(1 - \Gamma)(\bar{U}_t - \bar{U}_{nt})(\bar{V}_t - \bar{V}_{nt}) \quad (2)$$

Since the results from  $v'$  indicate the mean-step between  $\bar{V}_t$  and  $\bar{V}_{nt}$  is almost null, the last term of equation 2 is not expected to have a significant contribution on the overall Reynolds shear stress. The evolution of the conditionally sampled Reynolds shear stress,  $\overline{uv}$ , for the baseline case is shown in Fig. 7.

The non-turbulent contribution to the shear stress throughout the transition region is relatively small. This shows the weak correlation between the streamwise and cross-stream velocity fluctuations in the non-turbulent portions. The turbulent portion immediately increases above the wall shear and above the unconditioned result, obtaining a magnitude nearly three times the wall shear at station 05 ( $\Gamma = 0.05$ ). The peak magnitude remains at about three times the wall shear at station 06 ( $\Gamma = 0.50$ ) and then begins to decay, reaching a value of 1 by station 08 ( $\Gamma = 0.98$ ). This evolution of the turbulent shear indicates that the unconditioned values are not representative of the true turbulent

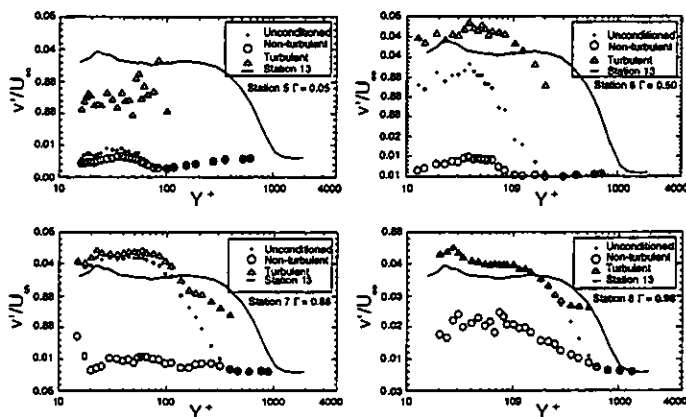


Fig. 4 Conditionally-sampled  $v'$  for the baseline case.

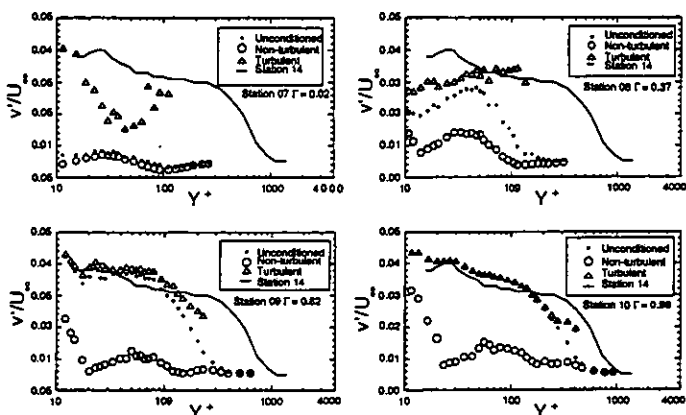


Fig. 5 Conditionally sampled  $v'$  for the K1 case.

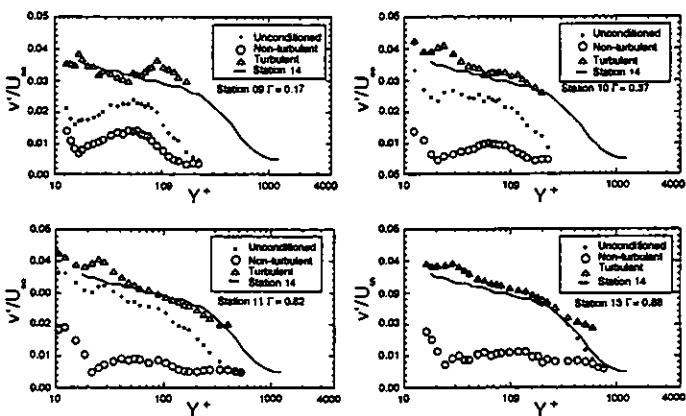


Fig. 6 Conditionally sampled  $v'$  for the K2 case.

shear through the transition process. To provide additional insight into the turbulent shear, the results for the baseline case are replotted in Fig. 8 but are normalized by the individual  $C_f$  values obtained for each portion (i.e., the turbulent and non-turbulent values shown in Fig. 4 of Part 1). By presenting the Reynolds shear stress in this manner, the peak magnitudes in the turbulent portion are significantly reduced. The peak magnitudes of  $\overline{uv}$  in the turbulent portion for stations 05 through 07 still exceed the wall shear but not by the magnitude previously seen in Fig. 7. For station 06 ( $\Gamma = 0.50$ ),  $\overline{uv}$  in the turbulent portion reaches a maximum of approximately 1.4 and occurs at  $Y^+ \approx 100$ , not at  $Y^+ \approx 40$  shown by the unconditioned portion. The trend of the Reynolds shear distribution in the turbulent portion for station 07 is similar to that observed in station 06 even though the unconditioned values are not similar. Note that the  $\overline{uv}/(U_\tau)^2$  values in the turbulent portion at station 7 in Fig. 8 become lower than the unconditioned values because the  $C_f$  values used in the turbulent portion in Fig. 8 are much higher than the unconditioned  $C_f$  values used in Fig. 7. For station 07 ( $\Gamma = 0.88$ ) the peak of  $\overline{uv}$  in the turbulent portion is 1.3 times greater than the wall shear. This supports the statement that the turbulent shear is generated within the turbulent portion of the flow and away from the wall at approximately  $Y^+=70-100$  and that the higher turbulent shear away from the wall is not due to the mean-step contribution.

Fig. 7 provides information of the absolute magnitude difference of  $\overline{uv}$  between non-turbulent and turbulent parts since a constant value of  $U_\tau$  is used for all three parts. Fig. 8 provides information of normalized  $\overline{uv}$  values relative to the shear wall shear stress of each part respectively. Both presentation methods are informative and provide physical insights to the evolution of turbulence transports in the transition process. However, limited by the paper length, only the second normalization method is used for the accelerating cases in this paper. The complete data presentation can be found in Keller's dissertation (1993).

Selected conditionally sampled results of the Reynolds shear stress for the accelerating cases normalized by the respective  $C_f$  values of each portion are shown in Figs. 9 and 10. For the K2 case (Fig. 10), comparison of  $\overline{uv}$  between the unconditioned and turbulent portions between station 10 ( $\Gamma=0.37$ ) and 11 ( $\Gamma=0.62$ ) reveals that the distribution of turbulent shear is more uniform

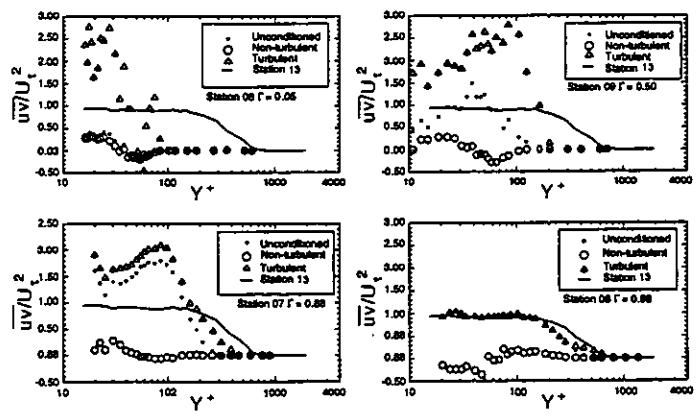


Fig. 7 Conditionally sampled Reynolds shear stress for the baseline case (normalized by unconditioned  $C_f$ ).

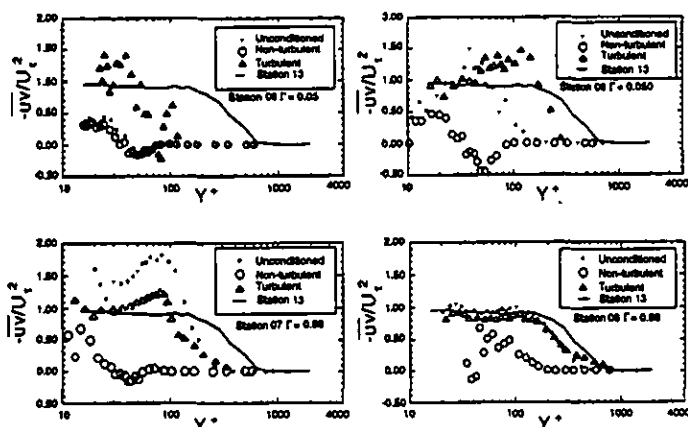


Fig. 8 Conditionally sampled Reynolds shear stress for the baseline case (normalized by individual  $C_f$  of each portion).

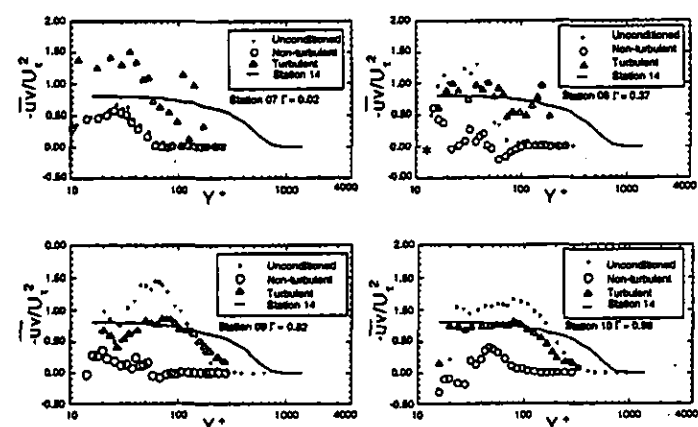


Fig. 9 Conditionally sampled Reynolds shear stress for the K1 case (normalized by individual  $C_f$  of each portion).

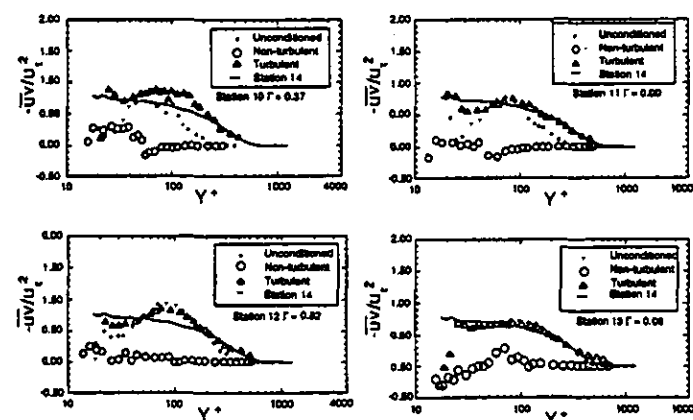


Fig. 10 Conditionally sampled Reynolds shear stress for the K2 case (normalized by individual  $C_f$  of each portion).

through the inner boundary layer for the turbulent portion than the unconditioned result. For example, in the inner boundary layer at station 10 ( $\Gamma = 0.37$ )  $\overline{uv}$  for the unconditioned data reaches a maximum value at  $Y^+ = 60$  and quickly decreases in magnitude as the wall is approached, while  $\overline{uv}$  in the turbulent portion remains at a relatively constant value. In the outer boundary layer, for  $Y^+ > 50$ ,  $\overline{uv}$  for the unconditioned data rapidly decreases to a zero magnitude by  $Y^+ = 200$ , whereas for the turbulent portion,  $\overline{uv}$  slowly decays in magnitude in the outer boundary layer. This difference is partly caused by the engulfing of the intermittent irrotational flow from the free stream. As transition progresses, these differences become less pronounced and  $\overline{uv}$  for the unconditioned data and the turbulent portion are nearly indistinguishable by station 13.

**RMS Temperature Fluctuations ( $t'$ ).** The conditionally sampled RMS temperature profiles, normalized by  $T_w - T_\infty$  for the baseline case are shown in Fig. 11. The profiles are similar to those observed in the  $u'$  profiles shown in Fig. 1. The non-turbulent portion exhibits a peak intensity of 0.045 at  $Y^+ \approx 35$  ( $y/\delta^* \approx 1.3$ ) at station 05 ( $\Gamma = 0.05$ ) which is slightly below the 0.05 peak value for the unconditioned result which occurs at the same  $Y^+$  location. For station 06 ( $\Gamma = 0.50$ ) the peak intensity for the non-turbulent portion increases to 0.075 and remains at  $Y^+ \approx 35$ . The peak magnitude for the unconditioned result is 0.12 at this station and occurs closer to the wall  $Y^+ \approx 15$  ( $y/\delta^* \approx 0.3$ ). In the late transition region, stations 07 through 08, the peak intensity in the non-turbulent part continues to increase in magnitude but does not migrate closer to the wall until station 08. For station 08 ( $\Gamma = 0.98$ ), the peak intensity in  $t'$ , similar to the result of  $u'$  for the non-turbulent portion, exceeds both the turbulent and unconditioned values near the wall. This can be contributed by the unsteadiness (not turbulence) of the highly-disturbed non-turbulent portion. For station 05 ( $\Gamma = 0.05$ ), the maximum value of  $t'$  in the turbulent part reaches 0.10 which is greater than the 0.05 reached in the unconditioned part for the same  $Y^+$  location. For station 06 ( $\Gamma = 0.50$ ), the peak magnitude in  $t'$  for the turbulent portion increases to 0.15 at  $Y^+ \approx 15$  ( $y/\delta^* \approx 0.3$ ) and still exceeds the unconditioned value. At station 07 ( $\Gamma = 0.88$ )  $t'$  in the turbulent portion for  $Y^+ < 40$  is slightly below the unconditioned result; this indicates a contribution from the step alternation in mean temperature. The near-wall peak of turbulent portion decreases in magnitude from station 07 to station 08. The secondary peak that was seen to occur at  $Y^+ \approx 200$  for the unconditioned result also occurs in both the non-turbulent and turbulent portions. This indicates that this second peak is not majorly caused by the mean-step contribution but rather is a direct result of the temperature fluctuation.

The conditionally sampled  $t'$  profiles for the accelerating cases are shown in Figs. 12 and 13. The effect of a favorable pressure gradient is seen to be most significant in the non-turbulent portion. For the K2 case, the broad peak in the  $t'$  profiles for the non-turbulent portion occurring at  $Y^+ \approx 40$  for station 09, continually increases in magnitude. At station ( $\Gamma = 0.62$ ), the peak intensity in  $t'$  occurs at  $Y^+ \approx 100$  and is approximately the same magnitude as both the turbulent and the unconditioned value. By station 13 ( $\Gamma = 0.93$ ) the peak intensity in  $t'$  for this region is

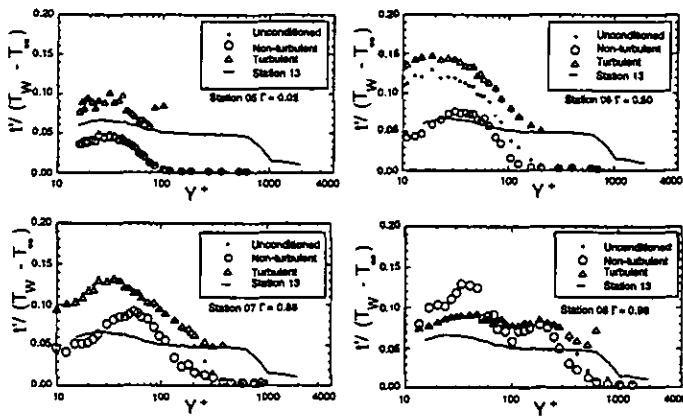


Fig. 11 Conditionally sampled RMS temperature for the baseline case.

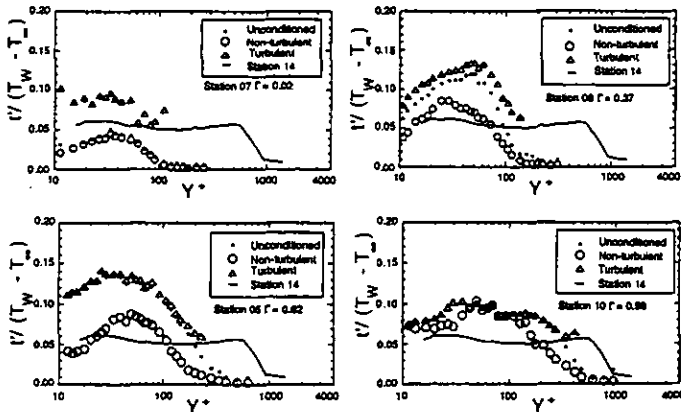


Fig. 12 Conditionally sampled RMS temperature for the K1 case.

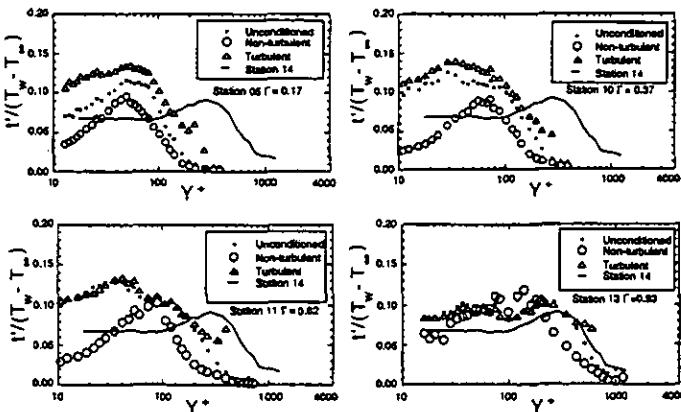


Fig. 13 Conditionally sampled RMS temperature for the K2 case.

greater than both the turbulent part and the unconditioned values. This behavior did not occur in the corresponding  $u'$  profiles where the fluctuations in the non-turbulent portion never exceeded the unconditioned or the turbulent part values in the K2 case. The exact reason for this phenomenon is not clear. Probably, this difference is caused by the fact that pressure gradients directly interact with the momentum transport but not with the thermal transport.

**Reynolds Heat Fluxes ( $\overline{ut}$ ).** The conditionally sampled streamwise Reynolds heat flux,  $\overline{ut}$ , for the baseline case is shown in Fig. 14. The peak intensity in the non-turbulent portion occurs at the same cross-stream location as was observed in the  $t'$  profiles. At station 05 ( $\Gamma = 0.05$ ) the magnitude of the peak intensity is approximately 3.5. By station 06 ( $\Gamma = 0.50$ ) this peak intensity in  $\overline{uv}$  increases to 7.0 and maintains this level until station 08 ( $\Gamma = 0.98$ ). For the turbulent portion,  $\overline{ut}$  exceeds the wall heat flux by more than a factor of 15 at station 05. By station 06 ( $\Gamma = 0.50$ ) this value has increased to over 20. The large values of convective heat transfer in the streamwise direction,  $\overline{ut}$ , are a result of the turbulent transport within the turbulent portions.

The conditionally sampled results of  $\overline{ut}$  for the accelerating cases are shown in Figs 15 and 16. The results indicate that the effect of a favorable pressure gradient is to increase the convective heat transfer in the streamwise direction,  $\overline{ut}$ , in both the turbulent and non-turbulent portions relative to the baseline case. The presence of a relatively large  $\overline{ut}$  value in the non-turbulent portion does not necessarily indicate that a significant turbulent transport of heat is occurring but only that  $u$  and  $t$  are correlated due to the unsteadiness of the flow. A second peak around  $Y^+ = 12.0$  appears downstream of station 11. The reason for this second peak in accelerating flow is not clear. The results of the cross-stream Reynolds heat flux,  $\overline{vt}$ , are not presented here due to a large uncertainty in  $\overline{vt}$  measurements, as discussed by Wang et al. (1992).

**Eddy Viscosity,  $\epsilon_M$ .** The results of the conditionally sampled eddy viscosity,  $\epsilon_M$ , normalized by the molecular viscosity are shown in Figs. 17 and 18. For the baseline case, the values obtained in the turbulent portion are larger than the unconditioned values but are significantly below the fully turbulent values obtained at station 13 (see Fig. 17). As  $K$  increases, both the turbulent part and the unconditioned  $\epsilon_M$  values decrease.

## CONCLUSION

A conditional sampling technique was employed to analyze the fluctuation quantities in the turbulent and non-turbulent parts of accelerated boundary layers undergoing laminar-turbulent transition on a uniformly heated flat plate. The results indicated that the increased magnitudes of the unconditionally sampled  $u'$  and  $t'$  were discovered to be a direct result of the fluctuations in the turbulent portions. The "mean-step" contribution to  $u'$  due to the alternating behavior between turbulent and non-turbulent flows were about 20% in the near-wall region but were negligible for  $Y^+ > 30$ . The peak intensity of  $u'$  and  $t'$  in the non-turbulent portion was suppressed at an earlier stage, as acceleration increased. The peak magnitude of  $\overline{uv}$  in the turbulent parts of the accelerating cases exceeded the wall shear but not by the magnitude seen in the baseline case. The

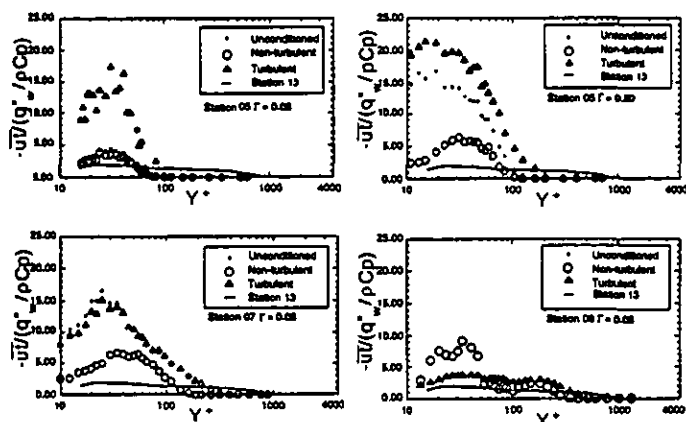


Fig. 14 Conditionally sampled Reynolds streamwise heat flux for the baseline case.

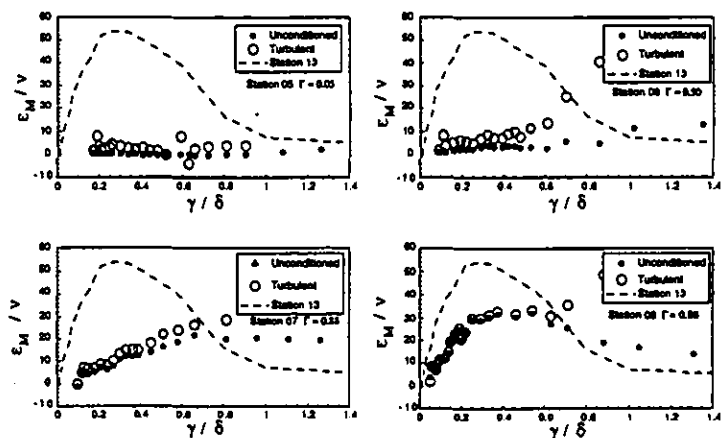


Fig. 17 Conditionally sampled eddy viscosity for the baseline case.

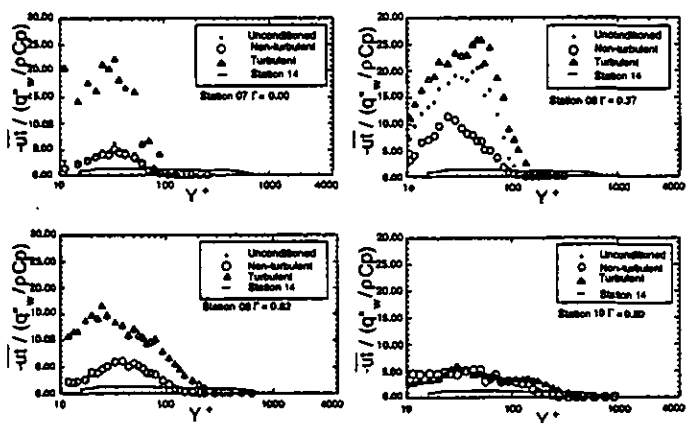


Fig. 15 Conditionally sampled Reynolds streamwise heat flux for the K1 case (in wall units).

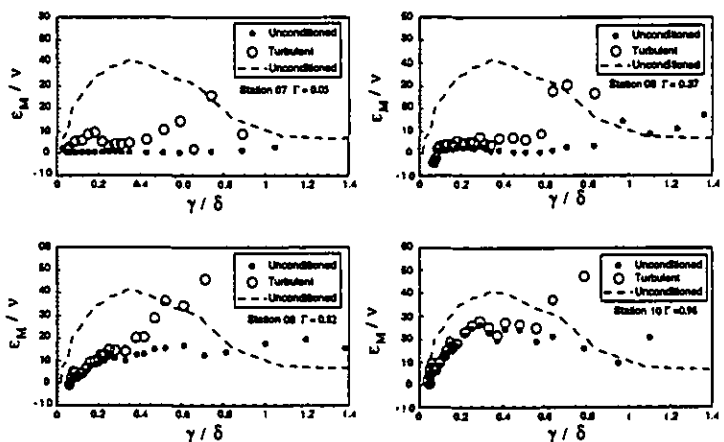


Fig. 18 Conditionally sampled eddy viscosity for the K1 case.

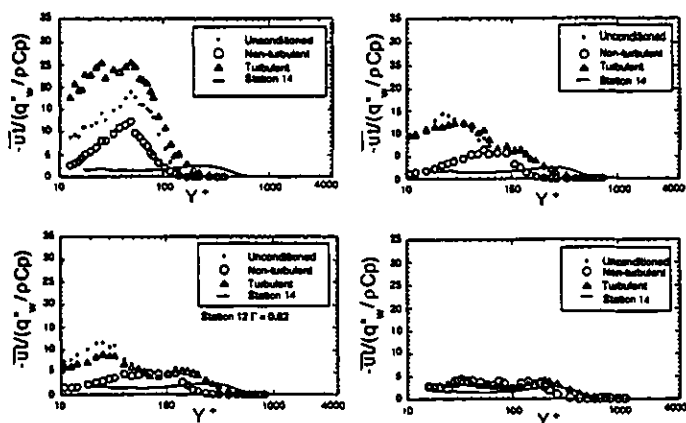


Fig. 16 Conditionally sampled Reynolds streamwise heat flux for the K2 case.

turbulent part  $\overline{uv}$  values were higher than the fully turbulent and unconditioned values in the inner boundary layer but lower in the outer boundary layer. The "mean-step" contribution to unconditioned  $\overline{uv}$  values was negligible. As acceleration increased,  $\overline{uv}$  in the turbulent portion was more uniformly distributed through the inner boundary layer than the unconditioned results.

In accelerating cases, the peak of  $v'$  of the turbulent portion reached the fully turbulent value in the middle of the transition at  $\Gamma \approx 0.5$  and changed little downstream. The effect of acceleration on non-turbulent portion  $v'$  is similar to non-turbulent portion  $u'$ . The unconditionally sampled RMS temperature fluctuations,  $t'$ , exceeded both the turbulent and non-turbulent values throughout most of the boundary layer. This indicated that a mean-step contribution to the large unconditioned  $t'$  values was not negligible. The effect of acceleration on  $t'$  was seen to be most significant in the non-turbulent portion. The streamwise Reynolds heat flux transport,  $\overline{ut}$ , increased as acceleration increased in both turbulent and non-

turbulent portions of the boundary layers. A second peak of  $u^+$  of the turbulent part at around  $y^+ = 120$  appeared as  $K$  increased.

For the baseline case, the values of eddy viscosity, obtained in the turbulent portion were larger than the unconditionally sampled values and were significantly below the fully turbulent values.

## ACKNOWLEDGEMENT

This research was sponsored by the Air Force Office of Scientific Research (Grant No. F49620-94-1-0126). The program manager was Dr. James McMichael.

## REFERENCES

- Blair, M.F., 1992. "Boundary-Layer Transition in Accelerating Flows with Intense Free-Stream Turbulence : Part 1-Disturbances Upstream of Transition Onset; Part 2-The Zone of Intermittent Turbulence," ASME Journal of Fluids Engineering, Vol. 114, pp. 313-332.
- Keller, F.J., 1993, "Flow and Thermal Structures in Heated Transitional Boundary Layers with and without Streamwise Acceleration," Ph.D. Dissertation, Department of Mechanical Engineering, Clemson University, Clemson, S.C.
- Keller, F.J. and Wang, T., 1996, "Flow and Thermal Behavior in Transitional Boundary Layers with Streamwise Acceleration," ASME Journal of Turbomachinery, Vol. 118, pp. 314-326.
- Kim, J., Simon, T.W., and Kestoras, M. 1994, "Fluid Mechanics and Heat Transfer Measurements in Transitional Boundary Layers Conditionally Sampled on Intermittency," ASME Journal of Turbomachinery, Vol. 116, pp.405-416.
- Kuan, C.L. and Wang, T., 1990, "Investigation of the Intermittent Behavior of a Transitional Boundary Layer Using a Conditional Averaging Technique," Experimental Thermal and Fluid Science, Vol. 3, pp. 157-170.
- Schubauer, G.B. and Skramstad, H.K., 1947, "Laminar-Boundary Layer Oscillations and Transition on a Flat Plate," NACA Report No. 909.
- Schubauer, G.B., and Klebanoff, P.S., 1956, "Contributions on the Mechanics of Boundary-Layer Transition," NACA Technical Note #1289, Supersedes NACA TN 3489.
- Sohn, K.H., O'Brien, J.E., and Reshotko, E., 1989, "Some Characteristics of Bypass Transition in a Heated Boundary Layer," Presented at the 7th Turbulent Shear Flow Symposium, pp. 2.4.1-2.4.6.
- Sohn, K.H. and Reshotko, E., 1991, "Experimental Study of Boundary Layer Transition with Elevated Free-Stream Turbulence on a Heated Plate," NASA CR-187068.
- Wang, T., Keller, F.J. and Zhou, D., 1992, "Experimental Investigation of Reynolds Shear Stresses and Heat Fluxes in a Transitional Boundary Layer," ASME HTD Vol. 226, Fundamental and Applied Heat Transfer Research for Gas Turbine Engines, pp. 61-70.
- Wang, T., Keller, F.J., and Zhou, D., 1996, "Flow and Thermal Structures in a Transitional Boundary Layer," Experimental Thermal and Fluid Science, Vol. 12, pp.352-363.